Macromolecules

pubs.acs.org/Macromolecules

Article

Impact of Chemically Specific Interactions between Anions and Weak Polyacids on Chain Ionization, Conformations, and Solution Energetics

Massimo Mella* and Andrea Tagliabue

Cite This: *Macromolecules* 2022, 55, 4533–4547

Read Online

ACCESS | Metrics & More | Article Recommendations | Supporting Information

ABSTRACT: The presence of salts in a solution containing weak polyelectrolytes is known to modify both their titration behavior and conformations due to electrostatic screening. Instead, little is currently known about the changes induced by chemically specific interactions (e.g., charged hydrogen bonds, c-H-bonds). To investigate this aspect, we simulated the titration of weak polyacids with a primitive model and Monte Carlo methods in the presence of monovalent salts whose anions are capable of forming c-H-bonds with associated acid groups. The interaction between anions and weak polyacids (e.g., poly(acrylic acid)) substantially hampers ionization at low pH despite the somewhat limited number of coordinated anions, whereas it has a limited impact once pH > pK_a + 2 due to a progressive anion decoordination. Importantly, the suppression of ionization appears extremely local in nature, with different chain segments differing in pK_a by up to 1.3 units. As for chain conformations, c-H-bonds reduce the average sizes of polyacids independently of their structure as a consequence of multidentate binding or multiarm coordination in starlike species. Analyzing the length of chain segments with all monomers coordinated or uncoordinated has also evidenced that anion binding is extremely local in nature. The energetic analysis of c-H-bond formation suggests that polyacid chemical potential may be strongly lowered (up to −0.7 kcal/mol per monomer), the impact of such results on a few phenomena relevant for the physical chemistry of polyacid-containing solutions being analyzed in some detail.

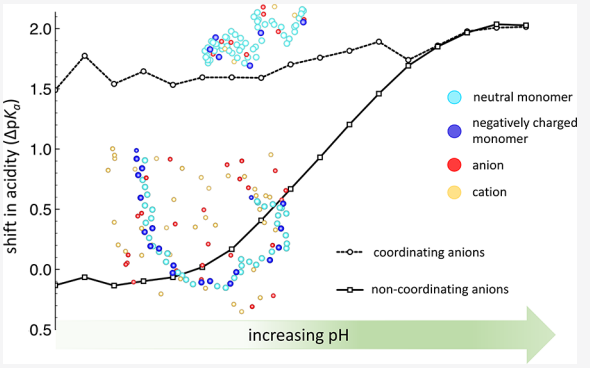

1. INTRODUCTION

Salt ions are known to influence the properties of polyelectrolytic chains in solution due to their Coulomb interaction with the chain charged moieties. Thus, the "end-to-end" distance in linear strong polyelectrolytes tends to decrease upon increasing the salt concentration (C_s), as it does the average gyration radius.[1,2] If chains represent the bristles of polymeric brushes, this effect results in a decrease in brush thickness[1,3,4] and, potentially, in a reduction in wettability of surface brushes.[5] A decrease in gyration radius upon increasing C_s is witnessed also in knotted and nonknotted ring polyelectrolytes,[6] the latter stimulus potentially modifying also the number of monomers involved in the knotted portion due to a reduction in Coulomb repulsion between essential crossings.[7] Divalent and trivalent salt ions, as well as hydrophilic macroions,[8] bearing charges of opposite sign than the polyelectrolyte affect the latter more markedly than monovalent ones,[9] so that packaging in tight vessels such as capsids may become possible.[10]

Compared to strong polyelectrolytes, a change in C_s affects chains composed of monomers with weak acid or basic activity in a few additional ways. Thus, an increase in salt content tends to facilitate monomer ionization, which is usually depressed compared to free monomers, as it helps reducing the impact of vicinal charges along the chains.[11−17] An even more marked effect of ionic force is evidenced when weak polyelectrolytic brushes are involved,[3,18] the Coulomb interaction with neighbor chains depressing ionization ever further. Apart from increasing the overall ionization degree (α), an increase in C_s strengthens also the natural tendency of weak polyelectrolytes to preferentially ionize at the extremities rather than around their chain midpoint. If multivalent ions with an opposite charge of the polyelectrolyte ones are present, the shift in ionization pK tends to be marked, easily reaching 1.5 pK units in the case of macroions such as micelles or solid nanoparticles.[19−26]

While the phenomena just recalled may be solely related to the fundamental characteristic of ions as charged mobile species, other effects can only be interpreted as due to

Received: December 30, 2021
Revised: April 8, 2022
Published: June 1, 2022

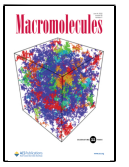

https://doi.org/10.1021/acs.macromol.1c02625
Macromolecules 2022, 55, 4533−4547

chemically specific interactions of salt ions with water or polyelectrolytes. Thus, the height of weak polybase brushes can be modulated by an appropriate selection of the salt anion, an increase in the chaotropic activity of the latter reducing the swelling following a decrease in pH.[5] A similar phenomenon appears to be induced by an increase in cation hydrophobicity for sodium polymethacrylate brushes.[27] Similarly, a marked modification of poly(acrylic acid) conformations at pH values sufficiently high to foster, at least, a partial ionization is induced by calcium ions,[28,29] a result interpreted as the consequence of Ca^{2+}-mediated bridging of carboxylate anions.[30,31] Other alkali-earth[32] and divalent transitions metal[33] cations (e.g., Pb^{2+} and Cu^{2+}) induce similar compaction behaviors. The latter, often, lead to polyelectrolyte aggregation, which, interestingly, appears also when sodium polyacrylate is mixed with Ag^{+} ions.[34]

Apart from the studies involving coordinating cations, recent work in the field of ion−polyelectrolyte interactions has suggested that other interaction modalities may also play a role in modifying the polyelectrolyte properties. For instance, the formation of nanosized aggregates appears to take place when poly(allylamine hydrochloride) (PAH) solutions is mixed with phosphate and polyphosphate anions.[35,36] As solution conformations of PAH change and nanoaggregates form even when adding monovalent $H_2PO_4^-$,[35] it seems likely that intermolecular forces other than electrostatic ones may play a role in driving the phenomenon. In particular, the formation of charged hydrogen bonds (c-H-bonds)[37] between the ammonium cation and the phosphate anions may help explaining the described behavior as well as the unusually low "slip plane" potential measured for polymersomes with PDMAEMA arms in the presence of a phosphate buffer with pH ∼ 8.[38] The formation of c-H-bonds between poly(acrylic acid) and the sulfonate group in sulfobetaine tensides (i.e., surfactants),[39,40] or between ω-carboxylic and carboxylate groups in surfactants,[41−45] was also suggested to be involved in lowering the critical micelle concentration of the mentioned surfactants.

As a consequence of the observations recalled above, we deemed as interesting to explore whether or not c-H-bonds between specific ions of monovalent salts and polyelectrolytic species may modify solution properties of the latter in a way that deviates from what is expected when only electrostatic interactions are accounted for. Thus, this work report on our efforts in this direction involving Monte Carlo simulations of a primitive model for salts and polyacids, the latter allowing the usage of a many-body potential model representing a few key features of c-H-bonds. In summary, we have determined the c-H-bond interaction strength leading to the formation of complexes between the salt anions and neutral polyacids. This allowed us also to gauge how the number of coordinated anions may depend on the structural features of the polyelectrolytic systems (i.e., linear, starlike, or composed of shorter oligomers) and on the concentration of monovalent salts as well as their impact on polymers' conformational properties. The dependence of the mentioned characteristics on pH (hence on the value of the ionization degree α) was explored via titration simulations, whose results allowed a precise characterization of the energetics involved in the coordination process when $\alpha \neq 0$.[46]

2. MODELS AND METHODS

2.1. Models. The cell model[47] was used to study properties of the systems under investigation; with this, polyelectrolyte monomers, their counterions, and salt ions are confined inside a spherical cell with radius R_{ext} = 159 Å and located at the origin of Cartesian axes.

Our systems consists of weak polyacid chains. The polyacids (pA) are such that N_{arm} linear arms depart from a neutral central monomer (nucleus) or contain N_{chain} free linear chains. Chains or arms contains L spherical weakly acidic monomers (beads) each; the maximum number of ionizable monomers thus is $N_{mono} = LN_{arm}$ or LN_{chain}. For convenience of discussion, we indicate polyelectrolytes with a nucleus, N_{arm} arms, and L monomers per arm (i.e., starlike) as $\mathcal{S}(N_{arm}, L)$. Similarly, systems composed of N_{chain} free chains are indicated as $\mathcal{L}(N_{chain}, L)$; thus, $\mathcal{S}(6, 10)$ is a starlike polyacid system with six arms, each composed of ten monomers.

Beads in each arm or chain are connected via harmonic springs; hence

$$U_{str} = \sum_{i}^{L-1} \frac{1}{2} k_{str}(r_{i,i+1} - \sigma)^2 \tag{1}$$

where $r_{i,i+1}$ is the distance between the monomer i and its first neighbor $i + 1$, $k_{str} = 200 k_B T/Å^2$ is the bonding force constant, σ = 3.85 Å is the equilibrium bond distance, and $k_B T$ = 0.5922 kcal/mol (0.9437×10^{-3} hartree or 299 K). This choice of parameters allows one a straightforward comparison with previous work of ours relevant for this study,[19,48,49] and *de facto* it was derived while modeling poly(ethylenimine) titration.[15] If present, the star nucleus has $\sigma_N = 2\sigma$.[19,48] Both σ and σ_N are also used to define the truncated (at the minimum, e.g., at $\sigma(2)^{1/6}$) and shifted Lennard-Jones potential employed to represent as soft spheres the N_{tot} particles composing our systems at every Monte Carlo step.

Acid monomers belonging to an arm or a chain may be neutral (q(mono) = 0) or singly charged (q(mono) = −1), their state varying during the simulation (*vide infra*); obviously, $N_{mono} = N_{mono,charged} + N_{mono,neutral} = LN_{arm}$ or LN_{chain}. The overall electroneutrality of the system is obtained with the presence of monovalent polyacid counterions (p-CI, q(CI) = +1) in the solution, so that $N_{CI} = N_{mono,charged}$. If the ionization of a neutral monomer is attempted by chance, a p-CI is randomly inserted to compensate for the total charge variation before computing the system energy; a randomly selected p-CI is instead eliminated if the charge of a monomer is neutralized (*vide infra* for further comments).

A uniform dielectric medium with water permittivity (ϵ_r = 78.3) screens the Coulomb interaction between charged objects, so that

$$U_{coul} = \sum_{i<j}^{N_{charge}} \frac{1}{\epsilon_r} \frac{q_i q_j}{r_{ij}} \tag{2}$$

Here, N_{charge} indicates the total number of charged objects. Notice that accepting the validity of eq 2, we implicitly assume that monomers and ions have identical permittivity as water (i.e., the solution permittivity is independent of the local composition).

The chemically specific interactions due to the c-H-bonds between neutral acid groups (e.g., carboxylic groups) and salt anions are described exploiting the same approach used to investigate the interaction between polyacids (or their anions) and the headgroups in zwitterionic micelles,[40,49], i.e., via a slightly modified version of our many-body (MB) interaction potential (see refs 20, 48, and 50). In short, (1) we consider

https://doi.org/10.1021/acs.macromol.1c02625
Macromolecules 2022, 55, 4533−4547

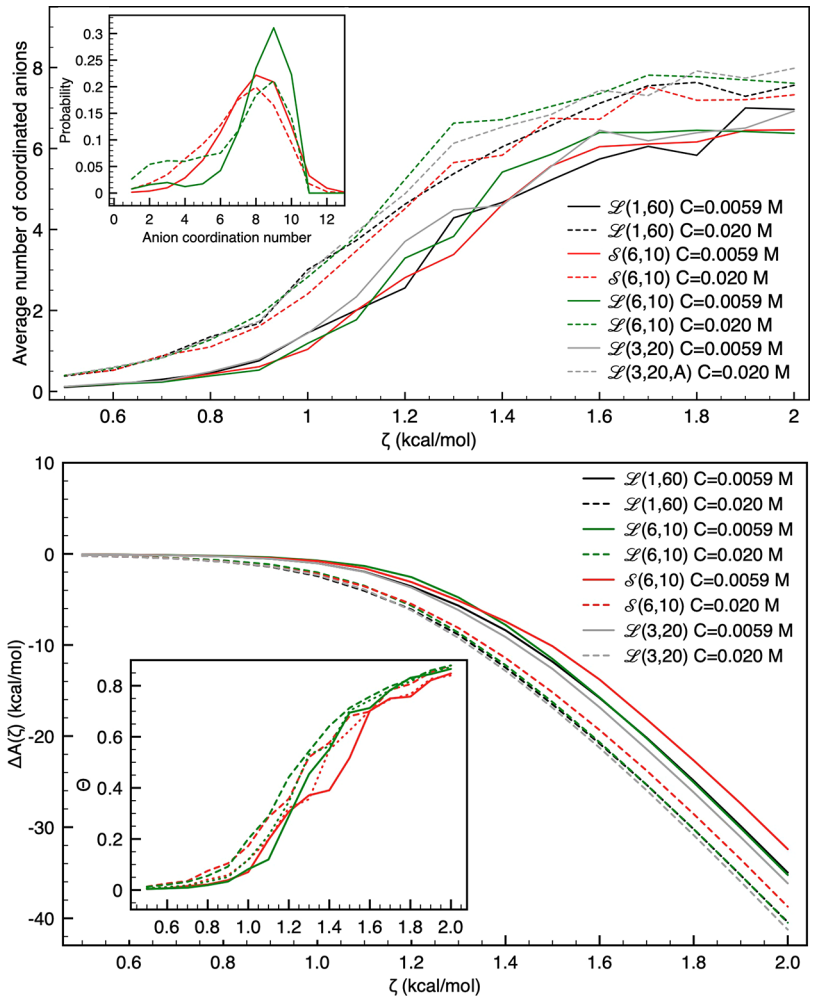

Figure 1. (top) Average number of coordinated anions as a function of ζ and C_s for the investigated systems. The distribution of number of c-H-bonds that each anion can form with polyelectrolyte monomers is shown in the inset for $\mathcal{S}(6, 10)$ and $\mathcal{L}(6, 10)$ (ζ = 2 kcal/mol). (bottom) Change in the Helmholtz energy $\Delta A(\zeta)$ of polyelectrolyte systems upon increasing ζ for the three C_s values investigated. The average fraction of monomers involved in c-H-bonds (Θ) as a function of ζ is also shown in the inset for $\mathcal{S}(6, 10)$ and $\mathcal{L}(6, 10)$.

the possibility that an anion and a neutral acid group on a monomer could be hydrogen bonded basing on their distance; (2) define a local number (ρ) of potentially interacting species satisfying the latter constraint for each monomer or anion; (3) consider only a subset of the possibly coordinating species basing on the maximum number of accepted or donated c-H-bonds dictated by the monomer or anion nature ($e(\rho)$), and (4) attribute a contribution to the system total potential energy due to c-H-bonds as $-\zeta e(\rho)$ (i.e., proportional to the total number of such interactions, $e(\rho)$). Parameters defining these MB interactions are therefore the cutoff radius (r_{MB}) below which species are considered interacting, the depth of the square-well interaction potential per interacting pair (ζ), and the maximum number of pair interactions that a weak electrolytic group (in our case, neutral carboxyl groups) and an anion can form ($n_{MB}^{(m)}$ and $n_{MB}^{(a)}$, respectively). In the present work, we have chosen $n_{MB}^{(a)} = \infty$, so that a limit to the number of c-H-bonds accepted by a salt anion is imposed only by excluded volume effects, and $n_{MB}^{(m)} = 1$; the latter choice is natural for a neutral carboxylic group, as it can donate only a single H-bond, while the former is compatible with the hydration number of SO_4^{2-} evidenced by molecular dynamics calculations.[51] Notice, however, that our model implicitly assumes freely orientable c-H-bond donors, a modeling choice that to some extent at least neglects an entropic contribution from conformational degrees of freedom;[52] this is to be considered somewhat subsumed in the bond strength, i.e., ζ.

To define the specific values of ζ and r_{MB}, we began recalling that the potential of mean force between acetic acid (representing the carboxyl bearing species) and the sodium salt of methanesulfonic acid[40] suggested ζ = 2 kcal/mol and r_{MB} = 5 Å to be sensible parametric choices largely independent of salt concentration. This notwithstanding, we explored the impact that a change in ζ value may have on properties such as the number of polyelectrolyte-coordinated anions running simulations with $\zeta \in [0.5, 2.0]$ kcal/mol (which is $\zeta/(k_BT) \in [0.85, 3.37]$). The latter results allowed, also, to determine the change in system Helmholtz energy induced by the possibility of forming c-H-bonds, thus better characterizing the thermodynamics involved in processes such as the mixing of polyelectrolyte and salt solutions.

2.2. Simulations. Monte Carlo simulations were used to sample the canonical distribution of the investigated systems. Simulations were performed so that the vast majority of the observables computed have associated statistical errors better than one part for hundredths; thus, we neglected to indicate

https://doi.org/10.1021/acs.macromol.1c02625
Macromolecules 2022, 55, 4533−4547

them for sake of clarity in our plots unless it was deemed necessary to highlight particularly "noisy" properties (e.g., the end-to-end distance). Random attempted displacements of particles Cartesian coordinates are accepted via the Metropolis−Hastings rule

$$P_{acc} = \min\{1, e^{-\Delta E/k_B T}\} \quad (3)$$

where ΔE represents the change in potential energy of the system. According to the constant-pH approach,[53] a random change in charge state of a titratable acid monomer is accepted by substituting ΔE in eq 3 with an energy change that accounts for the contribution of the proton chemical potential:

$$\Delta E'_{acid} = \Delta E \pm k_B T(\mathrm{pH} - \mathrm{p}K_a) \ln 10 \quad (4)$$

the plus sign being used when a monomer is protonated (association). For convenience of notation, we shall often use λ to indicate the difference $\mathrm{pH} - \mathrm{p}K_a$. Notice that ΔE in eq 4 is computed as energy difference between systems composed of a different number of particles, as p-CIs are introduced or deleted during the titration step to maintain the system electroneutral. Importantly, the constant-pH approach has a few limitations in the range of pH values that can be explored, as it does not explicitly introduce H^+ or OH^-, and such limits are related to their possible impact on the global electrostatic interaction if their concentrations become similar to the salt or monomer ones.[22,54] As indicated with some detail in the Supporting Information, our simulations never reach such problematic regimes.

At this stage, it appears important to stress that grand canonical titrations (as suggested in ref 55) should be employed if the salt defining the background ionic force shared counterion species with the titrant, as the chemical potential for the latter species may markedly depend on the extent of ionization. In the present circumstances, however, p-CIs for polyacids and salt anions are chemically different entities, and at least for the mentioned reason, such a prescription would not be necessary. This notwithstanding, the salt anion chemical potential would still be dependent on the polyelectrolyte ionization state due to the formation of c-H-bonds, and grand canonical simulations would, in principle, be needed unless a sufficiently high number of ion pairs is present. In the latter case, they would intrinsically act as salt bath, *de facto* eliminating the need for such a more complex simulation approach at the expenses of slightly longer simulation times. That this is exactly the case would be discussed at some length in section 3; here, we only mention that the number of coordinated anions has always been found to be a small fraction (0.15, at most) of the total anions present even at the lowest C_s simulated. Our choice of employing semi-grand canonical simulations rather than grand canonical ones is, thus, not expected to introduce any important bias in the results. To show that this is exactly the case, we rerun simulations for our worst possible cases, doubling the system volume (i.e., using R_{ext} = 200 Å); the results are shown and discussed in Figure S7.

3. RESULTS AND DISCUSSION

3.1. Dependence of the Extent of Anion Coordination on the c-H-Bond Interaction Strength and Its Consequences. As initial characterization of the consequences due to the presence of chemically specific interactions, we simulated several systems (i.e., $\mathcal{L}(1, 60)$, $\mathcal{L}(3, 20)$, $\mathcal{L}(6, 10)$, and $\mathcal{S}(6, 10)$) as a function of the interaction strength $\zeta \in [0.5, 2.0]$ kcal/mol; for the three values of C_s (namely 0.0059, 0.010, and 0.020 M[56]) used to explore the dependence on the latter quantity, we found ζ = 0.5 kcal/mol sufficiently low to maintain the systematic integration error in computing changes in Helmholtz energy below 0.1 kcal/mol. In all the simulations described in this section, polyacids were kept completely neutral (i.e., with a ionization degree α = 0) to maximize the number of possible c-H-bond contacts that each polyelectrolytic system can form.

Figure 1 shows a few results for the number of coordinated anions and the distribution of their coordination number as a function of ζ (top panel, the complete results being shown in Figure S1) as well the number of monomers involved in such coordination and the system Helmholtz energy change ($\Delta A(\zeta)$, bottom panel) for flexible polyacids.

As expected, the top panel of Figure 1 indicates a gradual increase of the number of coordinated anions upon increasing ζ, the capability of the various polyelectrolytes saturating around $\zeta \simeq 1.7$ kcal/mol with a maximum number of coordinated anions spanning the range 6.5−8.0 at ζ = 2.0 kcal/mol. While the number of coordinated anions does not depend markedly on the polymer structure (a maximum difference of roughly 0.5 been found for a chosen salt concentration), C_s appears to impact more strongly on the former quantity, the extent of such an impact depending somewhat on ζ itself. Thus, the increase in coordinated anions upon increasing C_s is larger when $1.0 \lesssim \zeta \lesssim 1.4$ kcal/mol than at the right extreme of the interval, where a partial saturation of the coordination sites has already taken place. Of importance with respect to our modeling choices, we also stress that the maximum number of coordinated anions remains small for all ζ and C_s values explored; hence, their solution concentration as free species is decreased by a small amount only. In turn, this fact indicates that the change of the anion chemical potential is limited in extent and thus would be also the number of inserted ion pairs from the salt bath to compensate for such a decrease. As indicated previously at the end of section 2.2, this conclusion is also supported by results obtained by doubling the system's volume (see Figure S7).

Apart from increasing the number of coordinated anions, changing C_s may also have an impact on the anion coordination modalities and, in particular, modify the number of monomers involved in the binding of a single anion. To demonstrate that this is just the case, the inset of the top panel in Figure 1 shows the distributions of the anion coordination numbers for $\mathcal{S}(6, 10)$ and $\mathcal{L}(6, 10)$ as a function of C_s when ζ = 2.0 kcal/mol, two systems for which the modifications induced by the latter variable is particularly evident. Thus, it is clearly seen that the probability of having low coordinated anions substantially increases upon increasing C_s, with well-developed tails or side peaks appearing at the highest salt concentration. The fact that this behavior is more marked for systems composed of short arms or chains is probably due to the involvement of chain termini, which are more numerous in the latter cases. In addition, the data shown indicate that the maximum coordination number (i.e., 12, as monomers and ions have similar radii) for an anion is only very rarely obtained during our simulations—a finding most likely due to the juxtaposition between effects due to thermal excitations (as $\zeta/(k_B T) \simeq 3$ when ζ = 2.0 kcal/mol) and geometrical constraints imposed by the polymeric nature of the acid.

https://doi.org/10.1021/acs.macromol.1c02625
Macromolecules 2022, 55, 4533−4547

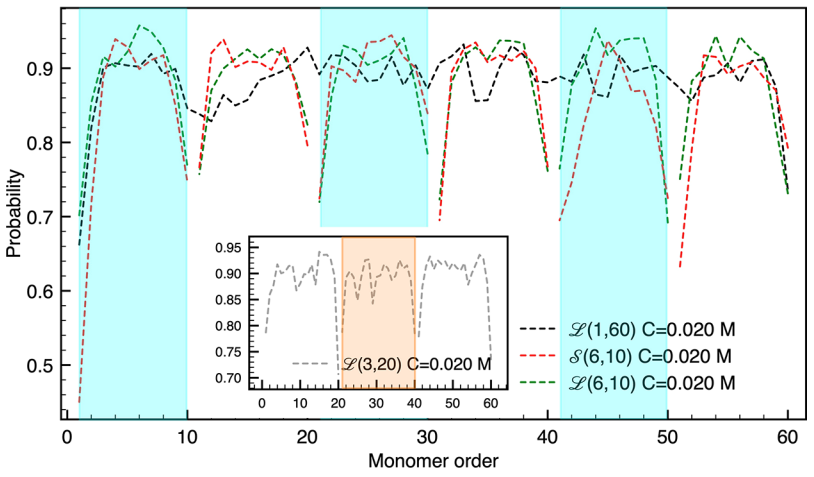

Figure 2. Probability for a monomer along a chain/arm to be involved in a c-H-bond with an anion when ζ = 2.0 kcal/mol and C_s = 0.02 M. Azure and orange shadings indicate different chains or arms in $\mathcal{S}(6, 10)$, $\mathcal{L}(6, 10)$, and $\mathcal{L}(3, 20)$. Notice the lower than average bonding probability for monomers 10−15 in $\mathcal{L}(1, 60)$.

The bottom panel of Figure 1 provides indication on the expected change in the polyelectrolyte Helmholtz energy due to anion coordination upon increasing the interaction strength ζ, which is the energetic counterpart of the change in number of monomers involved in c-H-bonds (see the inset in the bottom panel of Figure 1 for the fraction of coordinated monomers, Θ) as discussed at some length in the Appendix. As somewhat expected, Θ increases upon increasing ζ following a sigmoid-like behavior, the inflection point being located around ζ = 1.2 kcal/mol. This notwithstanding, Θ never reaches its theoretical maximum over the ζ interval explored despite the large amount of anions available in solution, a finding that is valid also for $\mathcal{L}(1, 60)$ and $\mathcal{L}(3, 20)$ not shown in the figure. To investigate the possible origin of the results just mentioned, Figure 2 shows the probability for each monomer to be coordinated to an anion; the latter clearly presents markedly lower values for monomers that lie close to a chain/arm end, indicating that such monomers are less likely, on average, to be involved in anion binding. In the case of $\mathcal{L}(1, 60)$, one also notices that a few contiguous monomers may present a somewhat lower coordination probability even though they are located far from the chain ends—an observation suggesting that the complexes formed are fluxional despite the strength of the interaction and that short chain fragments composed of noncoordinated monomers ("loops") may occasionally appear, reducing the overall coordination.

Starting from the latter observation, average lengths for loops, as well as for chain segments containing only coordinated monomers ("trains"), have been consequently estimated, and the results are discussed at some length in the Supporting Information (see Figure S2). Briefly, trains increase in length upon increasing ζ, while loops demonstrate an opposite behavior. As trivial as these indication may seem, a very rapid decrease in loop length suggests, however, that distal monomers may be involved in anion coordination when ζ is low. This idea is supported by the configurations shown in Figure 3, which also suggests a tighter coiling up of chains around anions upon increasing ζ; the latter occurrence is easily verified via the pair distribution functions between monomers shown in Figure 4, which clearly indicate an increase in the probability of finding two monomers as both neighbors and next-neighbors upon increasing ζ, the peak referring to the latter disposition nearly doubling in height as a consequence of increasing the interaction strength. Worth noticing, there is also the substantial increase in probability of finding two monomers belonging to different arms in $\mathcal{S}(6, 10)$ at distances in the ranges mentioned. In this case, this could only be due to an increase in the probability of having anions coordinated to two different arms. No similar features have been found, instead, for the $\mathcal{L}(6, 10)$ or $\mathcal{L}(3, 20)$ systems, their absence suggesting that no clustering between free chains takes place in the conditions chosen for this study.

The coordination of anions by neutral polyacids illustrated so far has, indirectly, the effect of conferring the latter with a net negative charge that, albeit lower than the one at α = 1, may somewhat modify its overall behavior in solution. *De facto*, the anion−polyacid complexes can be considered akin to negative macroions, with sizes that ought to depend on chains length and structure. Thus, they may form, for instance, coacervates when in the presence of polycations even though the pH is low enough to impede dissociation. The relatively high charge acquired may also be expected to impact on ion distributions attracting cations, which would tend to screen (at least partially) the complex negative charge, and repelling the noncoordinated salt anions. To appreciate the quantitative extent of this effect, the bottom panel of Figure 4 shows the ratio between cation−neutral monomer pair distribution functions computed with and without the possibility of forming c-H-bonds for a few selected cases. From the latter results, it becomes clear that cations progressively accumulate near the polyacid monomers upon increasing ζ, in good agreement with the increase in the average chain negative charge due to a more extensive anion coordination. Interestingly, the accumulation of cations seems to relatively weaken upon increasing the salt concentration despite an increase in anion coordinated and hence of the total charge acquired. Albeit part of the latter effect may be related to the fact that an increase in coordinated anions may impact on polyacid conformations[57] and, consequently, induce changes in the whole distribution, we suspect it to be mainly due to the stronger electrostatic screening that a more concentrated ionic solution can afford.

Other consequences on the behavior of polyacids solutions should also be expected as a result of anion coordination.

https://doi.org/10.1021/acs.macromol.1c02625
Macromolecules 2022, 55, 4533−4547

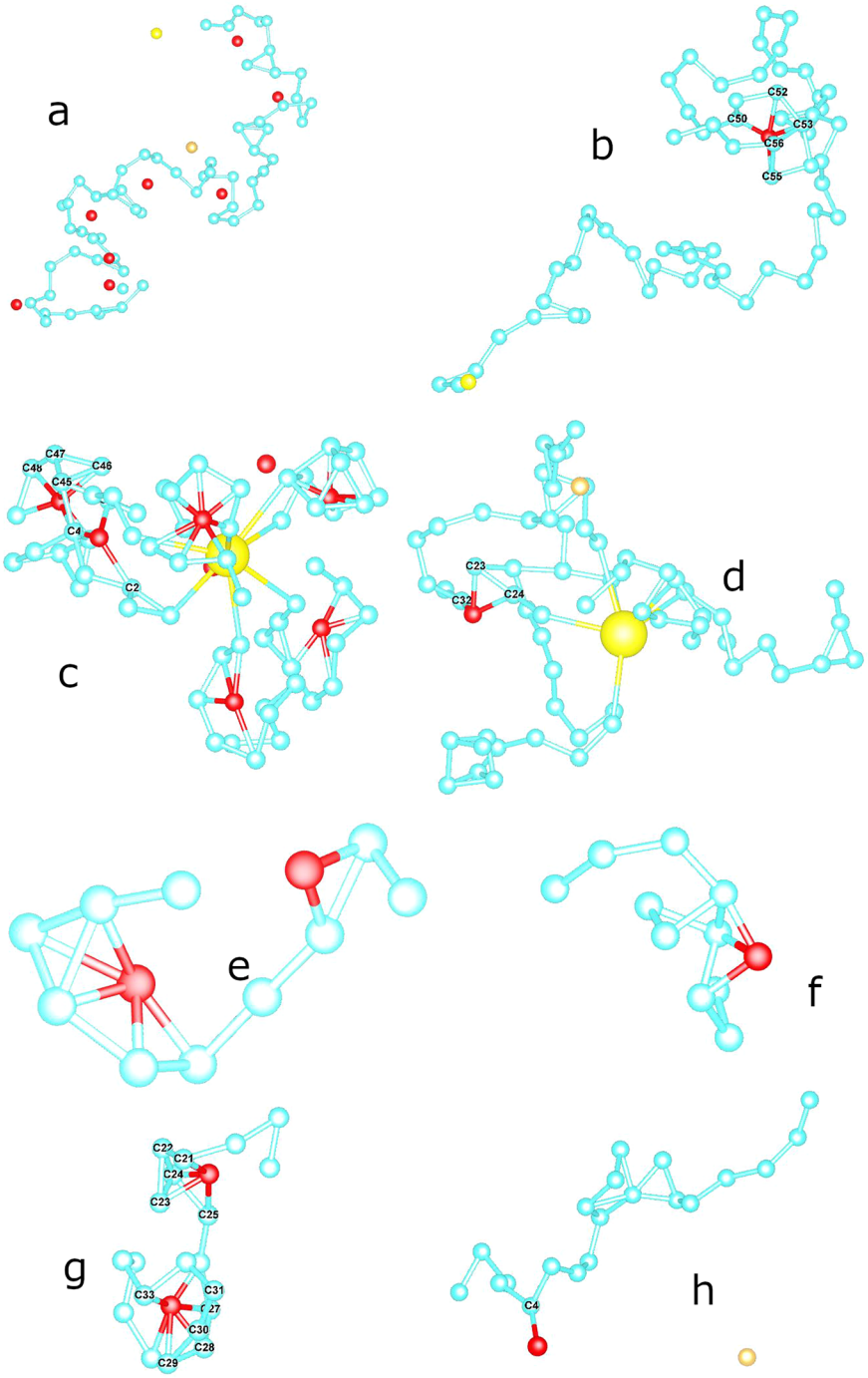

Figure 3. Configurations sampled for the studied polyacids when C_s = 0.0059 M, α = 0, and ζ = 0.8 (right column) or 2.0 kcal/mol (left column). From top to bottom: $\mathcal{L}(1, 60)$ (a, b); $\mathcal{S}(6, 10)$ (c, d); $\mathcal{L}(6, 10)$ (e, f); $\mathcal{L}(3, 20)$ (g, h). Monomer labels are also shown to localize coordination sites along chains in a few interesting cases. Color coding: light blue, neutral monomers; red, salt anions; light orange, salt cations; yellow, star nucleus.

Thus, the monotonic decrease of the Helmholtz energy of all systems upon increasing ζ and/or C_s clearly indicates the chemical potential of the solubilized polyelectrolyte decreases and, hence, that its solubility ought to markedly increase even when the strength of the c-H-bond interactions is substantially lower than the one estimated for the sulfonate/carboxylic acid interaction. Thus, considering ζ = 1.2 kcal/mol and C_s = 0.020 M, the Helmholtz energy of $\mathcal{L}(1, 60)$ in solution is lowered by 6.1 kcal/mol compared to the ζ = 0 or C_s = 0.0 M cases, so that the polyacid solubility ought to be increased by a factor $\exp[-\Delta A(\zeta)/RT] \simeq 29750$ at the conditions used for our simulations. Apart from the thermodynamical advantage afforded by the solubilized polyelectrolytes, it appears likely that also the aggregation of polyacids to form precipitation nuclei may be hampered by anion coordination due to the negative charge acquired by chains, their repulsion adding an enthalpic contribution to the entropy-related barrier that ought to be surmounted before the formation of a new phase could take place.

https://doi.org/10.1021/acs.macromol.1c02625
Macromolecules 2022, 55, 4533−4547

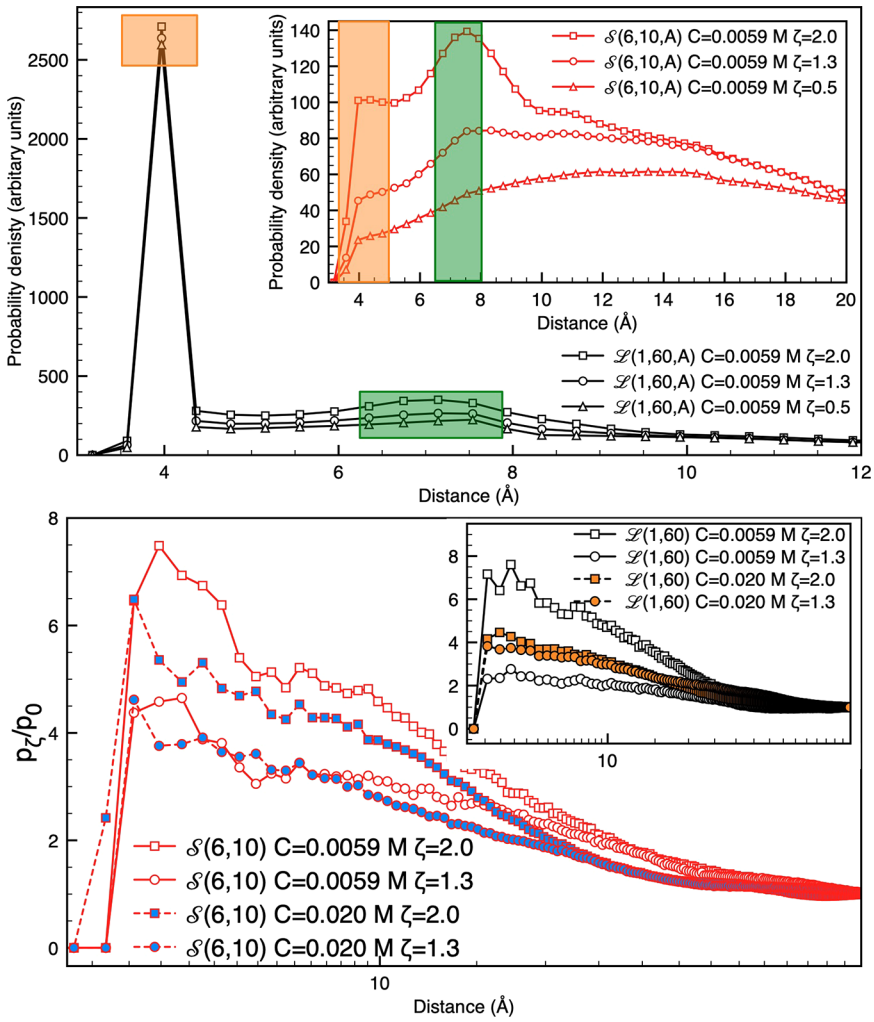

Figure 4. (top) Pair distribution function for neutral monomers in $\mathcal{L}(1, 60)$ when C_s = 0.0059 M, α = 0, and ζ = 0.5, 1.3, and 2.0 kcal/mol. The colored shadings highlight the range of distances pertaining to first (orange) and second (green) neighbors, as defined by the equilibrium distance of the stretching potential and twice the onset distance of the repulsive soft sphere potential. Inset: pair distribution function between monomers belonging to different arms on $\mathcal{S}(6, 10)$. (bottom) Ratio between neutral monomer−cation pair distribution functions computed for $\mathcal{S}(6, 10)$ with $\zeta \neq 0$ (p_ζ, with ζ = 1.3 and 2.0 kcal/mol) and ζ = 0 (p_0) for two values of salt concentration. The inset displays the same quantity for $\mathcal{L}(1, 60)$.

On a smaller scale compared to the latter phenomenon, the same behavior may impact on the aggregation of polymer-based surfactants to form micelles if the hydrophilic portion of the chains complexes anions. To show that, at least in principle, this may be the case, one may begin noticing that $\Delta A(\zeta)$ for $\mathcal{L}(6, 10)$ is always lower than for $\mathcal{S}(6, 10)$, the difference between the two values reducing in absolute value upon increasing C_s (e.g., −2.8 and −1.8 kcal/mol for respectively C_s = 0.0059 and 0.020 M). Hence, decameric chains are more stable when isolated than when bound to a nanoparticle, suggesting that anion coordination ought to destabilize micelles and, thus, increase the critical micelle concentration.

3.2. Titration Results. To gauge to what extent the acid dissociation is affected by anion coordination, Figure 5 shows $\Delta pK_a = pK_a^{eff} - pK_a$ as a function of λ = pH − pK_a for polyacids. Here, pK_{eff} is estimated by employing the Henderson−Hasselbach equation using the estimated α values (see Figure S3).

Beginning the discussion of our results with species for which ζ = 0 kcal/mol, we notice that, as usual, weak polyelectrolytes display an ideal behavior when $\alpha \simeq 0$ (or $\lambda \ll 0$); i.e., their dissociation conforms to the one of isolated monomers and $\Delta pK_a \simeq 0$, the small negative deviation being due to salt screening. However, ΔpK_a increases by two units upon increasing ionization over the $[-1, 2]$ interval of values for λ due to an increase in repulsion between charged monomers.

Turning to polyacids with ζ = 2 kcal/mol, it is apparent that the formation of c-H-bonds depresses ionization ($\Delta pK_a > 1$) when the pH is lower than pK_a, the shift in apparent pK_a depending somewhat on the polyelectrolyte structure. Thus, species with a lower number of monomers bound together present somewhat less marked shifts, probably due to the lower number of coordinated anions per independent chain and, hence, to a lower total negative charge. Upon increasing λ, ΔpK_a increases further, albeit only slightly, converging toward the values for the species with ζ = 0. The latter finding suggests that anions progressively decoordinate upon decreasing the moieties capable of donating c-H-bonds. Such decoordination should also be fostered by the repulsion with the negatively charged monomers, albeit the extent of the latter interaction may be somewhat weakened by the "condensation" of p-CIs

https://doi.org/10.1021/acs.macromol.1c02625
Macromolecules 2022, 55, 4533−4547

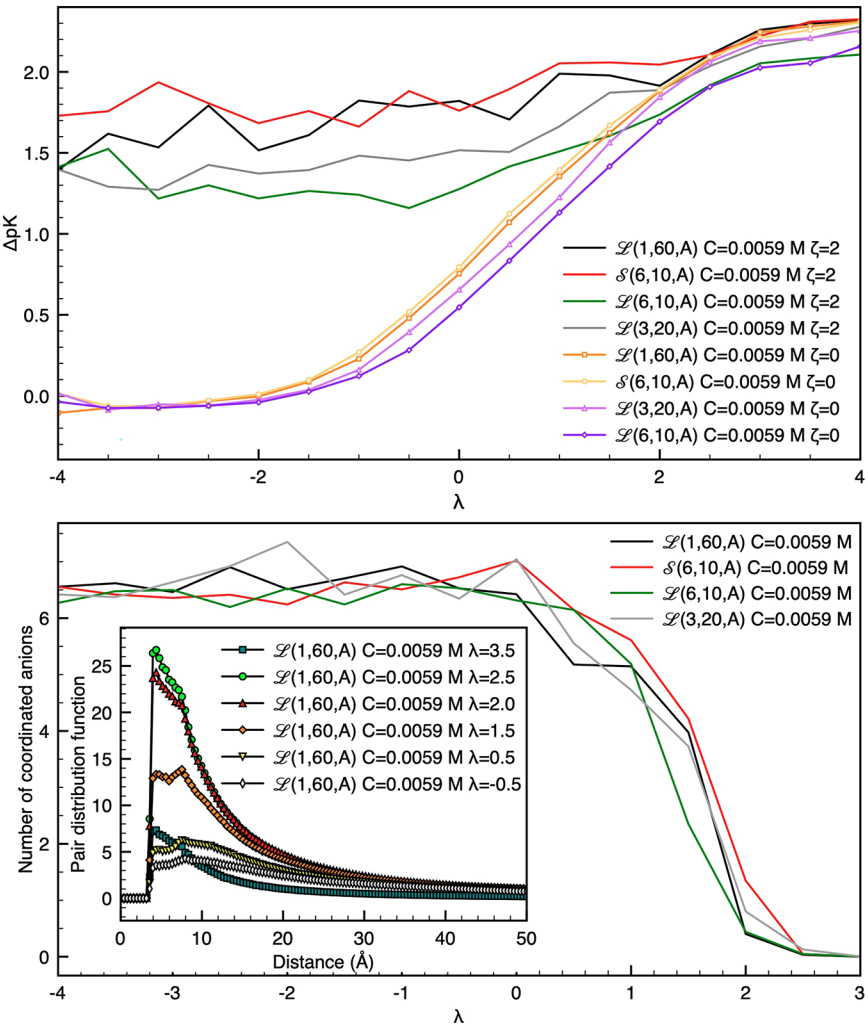

Figure 5. (top) Shift in pK_a^{eff} with respect to the value for isolated monomers as a function of the control variable λ for the investigated polyacids with ζ = 2.0 kcal/mol and C_s = 0.0059 M. Polyacids with ζ = 0.0 kcal/mol are also shown as a reference. (bottom) Average number of anions coordinated to polyacids (C_s = 0.0059 M) as a function of the titration control variable λ. Pair distribution functions between cationic species (i.e., p-CIs or salt cations) and neutral monomers for $\mathcal{L}(1, 60)$ are shown in the inset as a function of λ.

and salt cation on the polyelectrolyte itself. That anion decoordination and positive species condensation indeed take place is demonstrated by the average number of coordinated anions and pair distribution functions between neutral monomers and p-CIs plus salt cations (for $\mathcal{L}(1, 60)$) shown in the bottom panel of Figure 5. In the results, it is evidenced a decrease in number of bound anions over the interval $1 < pH - pK_a < 2$ and a strong increase in the probability of finding neutral monomers and cationic species in the range of distances that is characteristic of moieties in close contact. Importantly, the decrease in peak height shown by the pair distributions on going from λ = 2.5 to 3.5 is due to the marked decrease in number of neutral monomers along the chain. Increasing C_s to either 0.01 or 0.02 M only minimally impacts the behaviors shown in Figure 5, the only change worth noticing being a progressive shift to lower pK_a^{eff} of the curves in the top panel.

While the bottom panel of Figure 5 clearly indicates how, on average, varying λ impacts on the number of adsorbed anions controlling the number of monomers capable of c-H-bonding, it does not show if there are sections along chains from which anions detach preferentially—a scenario made likely by the possibility of finding differences in the electrostatic potential along a chain as a function of the position. To investigate if this is the case, the top panel of Figure 6 shows the probability for a monomer in $\mathcal{L}(1, 60)$ to be anion-coordinated when C_s = 0.0059 M as a function of λ. From the latter results, it is clearly evident that the anions tend to decoordinate preferentially from monomers located either to the extreme chain edges or in the central region upon increasing λ, while there is a clear preference for maintaining coordinated chain segments located only a few monomers (i.e., 5−7) from the polyelectrolyte termini. As one would expect, the latter results well correlate with the average monomer charge $\langle q \rangle$ along the chain (see right inset in Figure 6), as anion coordination is an important energetic contribution to the overall system's stability that is capable of suppressing both general and local ionization. Figure S4 allows one to gauge the local impact on ionization presenting $\mathcal{L}(1, 60)$ monomer's pK_a for selected λ values; differences of up to 1.3 units may be found for monomers in different chain positions.

The finding that anions prefer to remain coordinated *close* to, but *not at*, the chain edges may be rationalized as due to the juxtaposition between two effects, namely, the higher

https://doi.org/10.1021/acs.macromol.1c02625
Macromolecules 2022, 55, 4533−4547

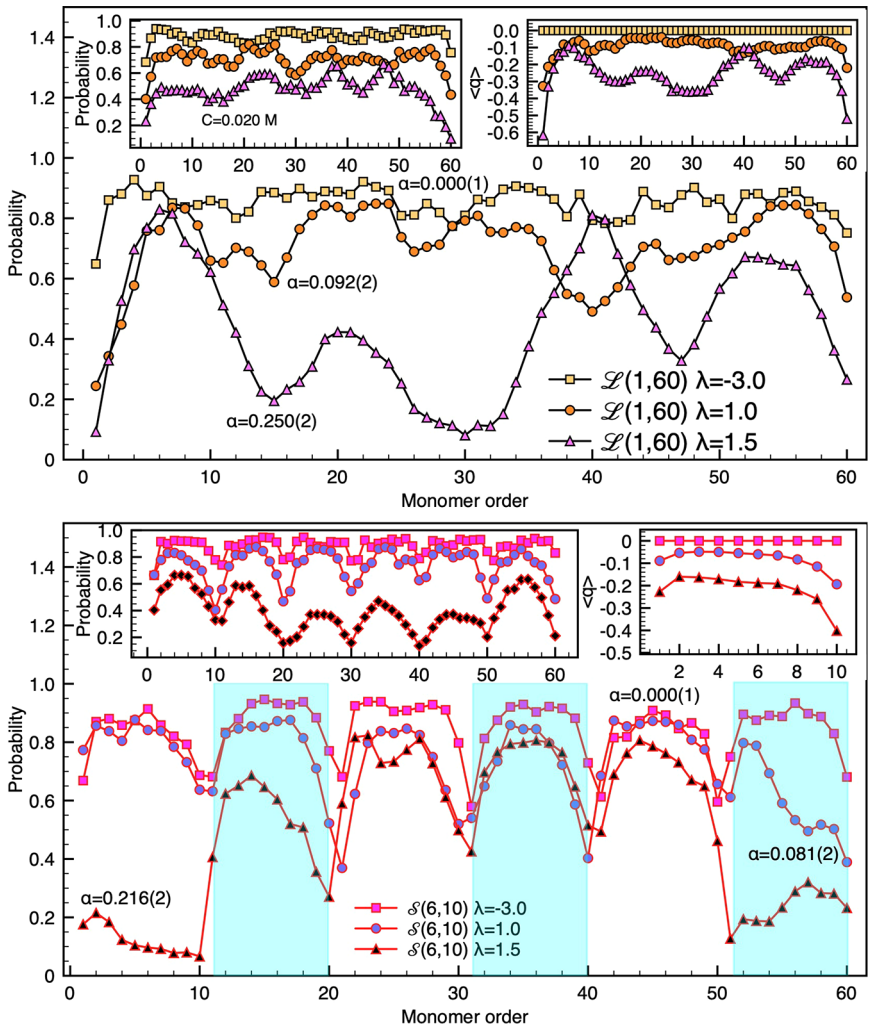

Figure 6. (top) Probability for monomers along $\mathcal{L}(1, 60)$ of forming a c-H-bond as a function of the control variable λ when C_s = 0.0059 M; the global ionization degree α is indicated alongside the curves, while the local ionization probability is shown in the right inset. The left inset is the c-H-bond probability for $\mathcal{L}(1, 60)$ when C_s = 0.020 M. (bottom) Probability for monomers along arms in $\mathcal{S}(6, 10)$ of forming a c-H-bond as a function of the control variable λ when C_s = 0.0059 M; the global ionization degree α is indicated alongside the curves, while the local ionization probability is shown in the right inset as an average over the six arms. Light blue shaded areas are used to indicate different arms. The left inset is the c-H-bond probability for $\mathcal{L}(1, 60)$ when C_s = 0.020 M.

ionization of terminal monomers (due to the lower repulsion experienced by the latter and the reduced coordination probability even when all monomer can form c-H-bonds; see Figure 2) and the tendency for coordinated monomers to have a lower ionization probability (hence, average charge) than uncoordinated ones. The latter behavior, *de facto*, partially neutralizes chain segments, which act as less repulsive "spacers" between more charged regions along the chain; this decreases the repulsion between charged monomers, with the terminal ones being the most advantageous to be "isolated" due to their higher than average ionization. As further support for this interpretation (see left inset in Figure 6), we mention that the coordination probability profile along the chain becomes substantially less jagged upon increasing the salt concentration up to C_s = 0.020 M, the stronger screening provided by the higher ionic force somewhat reducing the importance of isolating the more charged termini from the central part of the chain.

Turning to the structurally more complicated $\mathcal{S}(6, 10)$, the bottom panel of Figure 6 provides indications for an inhomogeneous behavior of the star arms, with monomers belonging to different arms demonstrating substantially different coordination probabilities. Such differences are particularly evident when λ = 1.0 and 1.5, the second value being located in the proximity of the inflection point in the curves describing the number of coordinated anions versus λ (see Figure 5). As counterpart, we have also found that arms may substantially differ in ionization at the same λ values (see Figure S5), with more ionized arms coordinating less anions; the same happens for chains in $\mathcal{L}(3, 20)$ or $\mathcal{L}(6, 10)$. A similar behavior has already been highlighted for starlike polyacids in the presence of oppositely charged macroions[19] and zwitterionic micelles,[40] the surfactant headgroups in the latter being allowed to c-H-bond with associated carboxylic groups, both cases presenting substantially different ionization and adsorption probability for different arms (see also ref 21). In this specific case, the rational of the mentioned behavior may be related to the fact that once an arm has begun losing c-H-bonds due to its partial ionization, it becomes less hindered to further increase its ionization compared to arms that

https://doi.org/10.1021/acs.macromol.1c02625
Macromolecules 2022, 55, 4533−4547

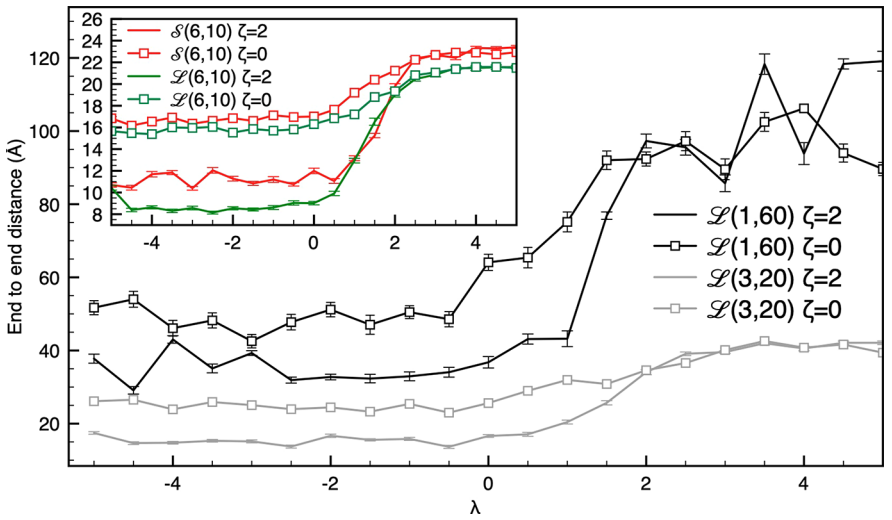

Figure 7. Average "end-to-end" distance for chains or arms in the studied systems as a function of the variable λ when C_s = 0.0059 M. Systems with ζ = 0 kcal/mol are also shown as a comparison. The equilibrium contour length for chains with L = 10, 20, and 60 are respectively, 34.7, 73.2, and 227.2 Å.

coordinate more anions. This is due to the possibility of relocating the still adsorbed anion further away from the charged monomer without loosing much c-H-bond interaction energy. In particular, the anion would "roll" closer to the nucleus. While entropic effects somewhat contrast the asymmetrization (more microstates are accessible to the system if charges are homogeneously distributed), they do not completely impede asymmetric fluctuations. To show that this is the case, we estimated the relative probability of having a single ionized monomer per each of six arms composed of ten monomers versus a situation in which two arms have exchanged a neutral monomer with a ionized one leaving the others unchanged; it turns out that the former microstate is only twice as likely than the second. Similarly, even more extreme cases do not particularly differ in terms of their relative probabilities. Thus, it appears, once again, that average properties of weak polyelectrolytes may not correctly represent their behavior, the probability distributions from which they are computed presenting, at least, long tails or being occasionally bimodal.[58]

To further investigate the coordination characteristics of c-H-bonding polyelectrolytes and their evolution as a function of the change in solution acidity, we have computed the average train and loop lengths versus λ and found, as expected, a decrease (increase) of the former (latter) upon increasing λ. While a more detailed discussion is provided in the Supporting Information (see Figure S6 and associated analysis), it is worth reporting that train length is quite more sensitive to a limited increase in ionization degree than the loop length—a feature that we interpret as related to the formation of isolated "coordination holes" due to dissociation and whose impact is to lower the probability of finding long sequences of coordinate monomers.

The shortening of trains, and the simultaneous freeing of portion of chains or arms, upon increasing λ should be expected to substantially impact on the conformation properties of the studied polyelectrolytes, especially considering that it happens concomitantly with the ionization of the latter, a phenomenon well-known to be the driving force for polymer straightening,[14,57−65] ring widening,[6] and the tightening[6] or localization of knots.[7] To gauge the quantitative aspects of such behavior, Figure 7 shows the average "end-to-end" distance for chains or arms in the polymeric systems as a function of λ. As expected, all cases present a more or less sudden increase in their length upon increasing λ, which appears in a range of values for the latter variable compatible with the one related to the increase in ionization (see Figure S3) as well as the one where decoordination of anions takes place (Figure 5). Given the discussion of the results presented so far, it appears thus evident that anion coordination also impacts on both local due to the involvement of contiguous monomers in their chelation (see the top panel of Figure S6), and global conformation, as it reduces the average polymer extension by at least 30% compared with the ζ = 0 kcal/mol cases. Also interesting is the fact that the decoordination-induced elongation shifts its onset progressively toward higher λ values and becomes relatively more marked upon increasing L. These traits appears to be easily rationalized by juxtaposing, again, the nearly identical number of coordinated anions for all studied systems when α = 0 with the decreasing average train length upon decreasing L. In other words, longer chains afford a higher number of consecutive monomers "hugging" an anion, *de facto* shortening more the effective chain length that shorter species do, as it is made substantially apparent in Figure 3, and requiring a lower proton chemical potential (i.e., higher pH or λ) to force the complete cleavage of c-H-bonds and, hence, re-elongation.[66]

3.3. Impact on Solution Thermodynamics of Polyelectrolyte Ionization. As a final aspect of the investigated systems worth studying, we recall our mentions for the possible impact that anion coordination via c-H-bonding could have on polymer solubility, precipitation, and, if part of the hydrophilic headgroup of a tenside, the critical micelle concentration of the latter species. As coordination is λ-dependent, its impact may also be modulated by the latter variable. Using systems with ζ = 0 kcal/mol as reference, we thus estimate the change in Helmholtz energy ($\Delta_{\zeta=0\rightarrow 2}A(\mathrm{pH}^*)$) for any of our polyelectrolytes due to the possibility of coordinating anions over the interval of λ values covered by our titration simulations; such a quantity represents the incremental stabilization that our systems gain when in solution due to the formation of c-H-bonds, and it is computed exploiting the thermodynamical

https://doi.org/10.1021/acs.macromol.1c02625
Macromolecules 2022, 55, 4533−4547

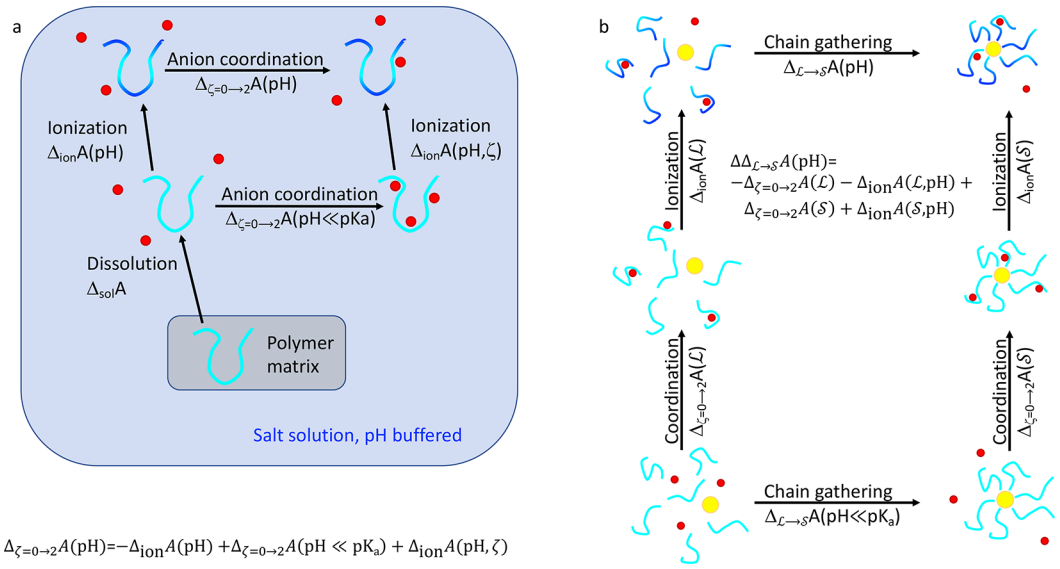

Figure 8. Paths decomposing (a) the dissolution process of a polyacid from its solid (with or without the possibility of forming complexes with the anions) and (b) the steps contributing to the Helmholtz energy change ($\Delta_{\mathcal{L}\to\mathcal{S}}A$) due to the formation of $\mathcal{S}(6, 10)$ from $\mathcal{L}(6, 10)$ when $\zeta \neq 0$ and the chains are, at least, partially ionized.

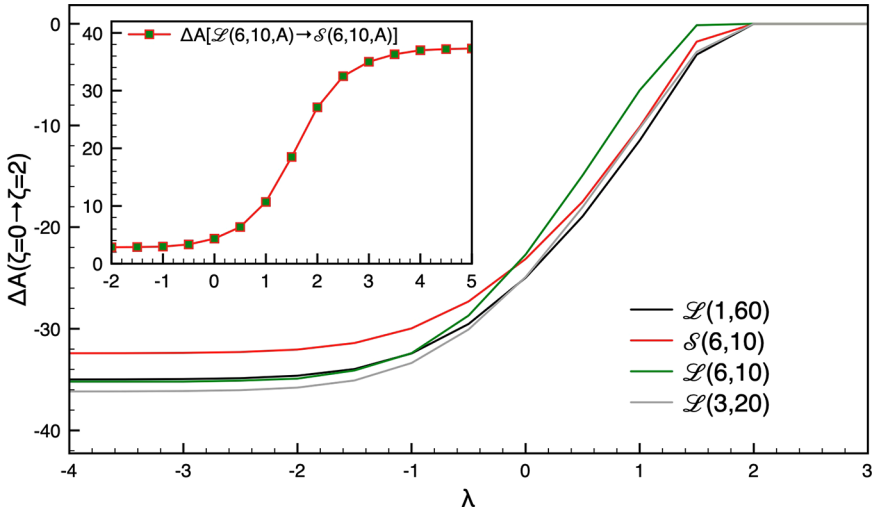

Figure 9. Difference in Helmholtz energy ($\Delta_{\zeta=0\to 2}A(pH)$, in kcal/mol) for structurally identical polyelectrolytes with ζ = 0 or 2 kcal/mol values as a function of λ when C_s = 0.0059 M. The inset shows, instead, an estimate for joint electrostatic and coordination components of the reversible work needed to gather six decameric arms around a central neutral nucleus (i.e., transforming $\mathcal{L}(6, 10)$ into $\mathcal{S}(6, 10)$).

path presented in the left panel of Figure 8. Notice that, employing eq 5 in the Appendix to estimate the change in polyelectrolyte Helmholtz energy ($\Delta_{ion}A(pH^*)$) due to the ionization fostered by a change in λ, estimating $\Delta_{\zeta=0\to 2}A(pH^*)$ via the proposed path requires the usage of information already available (i.e., $\Delta A(\zeta)$ in Figure 1 and data from the titration simulations by means of which the results discussed in this section were produced). Values of $\Delta_{\zeta=0\to 2}A(pH^*)$ for all the investigated systems when C_s = 0.0059 M are shown in Figure 9.

As clearly visible, the stabilizing effect of anion coordination decreases upon increasing λ, the onset of the latter trend being substantially independent of the structural details of the polyelectrolytes and located around $\lambda \simeq -2$. We notice, instead, that the latter value is substantially lower than the one found for the onset of anion decoordination (i.e., $\lambda \simeq 0$, see Figure 5), suggesting that it ought to be due to differences in $\Delta_{ion}A(pH^*)$ that are only related to the higher ionization of species with ζ = 0 kcal/mol (see Figure S3). With respect to the impact of polyelectrolyte structures, we notice that reducing chain length has a marked effect on $\Delta_{\zeta=0\to 2}A(pH^*)$, the system stabilization decreasing more the smaller L once $\lambda \geq -1$. Considering that the average number of coordinated anions by linear polyelectrolytes as a function of L begins to differ only once $\lambda \geq 1$ (see Figure 5), the substantially higher $\Delta_{\zeta=0\to 2}A(\lambda)$ seen for $\mathcal{L}(6, 10)$ is most likely due to the substantially higher ionization of the species with ζ = 0 kcal/mol compared to the longer linear counterparts. This is clearly evident in Figure S3, from which one notices that the same trend is present also when ζ = 2 kcal/mol. As for cases with higher C_s (not shown), we found results similar to the one displayed in Figure 8, the only differences being a more negative value for $\Delta_{\zeta=0\to 2}A(\lambda \ll 0)$ (due to the larger fraction of coordinated monomers) and a more rapid increase upon

https://doi.org/10.1021/acs.macromol.1c02625
Macromolecules 2022, 55, 4533−4547

increasing λ. The latter finding is easily justified by the fact that while increasing C_s increases ionization for all species thanks to the salt screening action, it does more for the polyelectrolytes with $\zeta = 0$ kcal/mol due to the mass effect on the number of coordinated anions and the consequent increase in electrostatic repulsion with charged monomers.

With respect to the possibility of bring together six decameric chains around a nucleus, a process previously indicated as akin to the micellization of surfactants with hydrophilic polymeric headgroups, the latter finding, thus, indicates that $\Delta_{ion}A(pH^*)$ for $\mathcal{L}(6, 10)$ is always more negative than for $\mathcal{S}(6, 10)$ when the species are capable of c-H-bond anions. Thus, one should expect the reversible work needed for the $\mathcal{L} \rightarrow \mathcal{S}$ process to increase upon increasing λ, the energetic impact involved in bringing together chains that are, at least, partially ionized probably becoming the key factor in defining the critical micelle concentration. Indeed, by using the thermodynamic path shown in the right panel of Figure 8 to analyze the mentioned process, one could estimate the impact of ionizing c-H-bonding chains in the $\mathcal{L} \rightarrow \mathcal{S}$ process with respect to the case involving chains with $\alpha = 0$ and $\zeta = 0$ kcal/mol computing the algebraic sum of the Hemlholtz energy changes taking place upon increasing both ζ and λ (i.e., the "vertical" steps, $\Delta\Delta_{\mathcal{L}\rightarrow\mathcal{S}}A(\lambda)$). The latter estimate indicates that the reversible work needed to form micelles is increased by up to 34.5 kcal/mol upon increasing λ and, hence, α when $\zeta = 2$ kcal/mol (see Figure 9). Assuming the aggregation of neutral non-c-H-bonding chains as reference, $\Delta\Delta_{\mathcal{L}\rightarrow\mathcal{S}}A(\lambda)$ can be used to gauge the impact of ionization on the critical micelle concentration as a function of λ via $\mathrm{cmc}(\lambda)/\mathrm{cmc}(\lambda \ll 0) = \exp[\Delta_{\mathcal{L}\rightarrow\mathcal{S}}A(\lambda)/(N_{agg}RT)]$, with N_{agg} being the aggregation number.[67−69] As $N_{agg} = 6$ for $\mathcal{S}(6, 10)$, our results thus suggest that the increase in cmc due to both anion coordination and ionization varies roughly in the interval 2−16000 as a function of λ, the upper limit being dictated only by repulsion between fully ionized arms. Of course, the latter value should be expected to be too high to adequately represent the impact of ionizing polymeric headgroups of realistic surfactants as, first, N_{agg} is too low and, second, the nucleus in $\mathcal{S}(6, 10)$ is very small compared to the core of micelles composed of tensides such as sodium dodecylbenzenesulfonate. Apart from the size difference just mentioned, it is also important to stress that other physical effects are not included in our model, among which the disruption of the water hydrogen-bonding network due to salts (the model describes the solvent as a continuum dielectric) or effects due to the translational entropy of solvent molecules; because of this, our analysis on how cmc may depend on λ provides indications on only a contributing effect.

4. CONCLUSIONS

In this work, we have exploited Monte Carlo simulations in both the canonical and semi-grand canonical ensembles to investigate weak polyacids in the presence of a salt whose anions can c-H-bond to undissociated acid groups. We explored how anion coordination depends on the salt concentration, the polyacid structure, and the c-H-bond interaction strength. We have characterized the latter relationships in terms of the average and distributions of coordination numbers, the length of chain trains and loops, and the preferential localization of anions along chains or arms as well as with respect to the overall influence on the energetics of polyacids in solution. In substance, it emerges that even c-H-bonds of moderate strength may have a deep impact on polyacid properties, reducing their size, increasing their solubility, potentially hampering their precipitation, or allowing the formation of coacervates with strong polycations even though the solution pH does not allow the dissociation of acid groups.

As c-H-bond formation relies on the availability of undissociated acid groups, the impact of such interaction is controlled also by the chemical potential of solution protons; we thus exploited semi-grand canonical (constant-pH) simulations to induce ionization as if in equilibrium with a proton bath. As it may have been expected, increasing anion coordination substantially decreases the acid strength of monomers. Conversely, reducing the proton chemical potential induces anion decoordination, which takes preferentially place in chain regions whose ensuing negative charge has a weaker impact on the overall systems energetics and fosters polymer elongation due to the appearance of longer sequences of uncoordinated monomers as well as the decrease in length of chain segments whose monomers are *all* embracing anions. If systems are composed of several fragments, we also noticed that an apparently independent mixture of coordinated and completely uncoordinated arms or chains is present when the systems are only partially ionized, a finding suggesting that the pH-dependent coordination of anions should not be considered as a "mean-field" effect but rather as due to the overlap of chains with fairly different properties. This consideration is also valid for the ionization itself, the less ionized fragments being the ones capable of coordinating a higher number of anions. It thus appears confirmed that "annealed" (i.e., weak or charge-regulating) polyelectrolytes composed of several fragments do not usually conform to a common average chain behavior (as suggested by Monte Carlo simulations performed by Stornes et al.[21]), a characteristic that could be used, for example, to desymmetrize arms in starlike species as already suggested basing on simulation results.[19,40] From the energetic standpoint, instead, we obtained indications for a substantially higher water solubility of polyacids capable of forming c-H-bonds with respect to their non-c-H-bonding counterparts over a fairly wide interval of pH values; the upper limit of the latter is clearly defined by the minimum number of undissociated acid groups needed to coordinate at least one anion.

Even though the main aim of this work was to explore polyacid−anion aggregation in its fundamental aspects, there are a few applications of our results that appear worth mentioning. For instance, coacervates obtained by mixing at low-pH polycations, polyacids, and anions coordinating the latter may have properties that differ substantially from the ones of material produced by mixing *only* polycations and polyanions, as the overall conformation of the negatively charged species would be quite different. Besides, the negative charge brought by the coordinated anions to the polyacids ought to be expected to be fairly mobile, a property that may confer to the coacervate a lower viscosity or even a better self-healing capability. Obviously, such features would be modified by an increase in pH, the monotonous increase in the chain overall negative charge easily estimated by our results fostering progressively stronger interactions between oppositely charged polyelectrolytes.

https://doi.org/10.1021/acs.macromol.1c02625
Macromolecules 2022, 55, 4533−4547

Inspired by our previous work on polyacids/zwitterionic micelles aggregates and by the general knowledge that strong polyelectrolytes are capable of reducing the cmc of oppositely charged surfactants (e.g., see refs 67−70 for modeling results and ref 71−73 for experimental results), one may also consider that anion−polyacid complexes could also have a cmc-lowering effect that otherwise would not be present at low pH unless the polyacid was markedly hydrophobic (e.g., see ref 39 for isothermal titration calorimetry results). The latter option, however, could be detrimental to an intended application, as the interface between a micelle and the water solution may become sufficiently less hydrophilic to foster aggregation with other species present in solution. Besides, the markedly lower charge that polyacids acquire upon anion coordination compared to their maximum ionization may be exploited to somewhat limit the decrease in cmc; obviously, the same goal may be reached by using copolymers with a lower charge density (e.g., inserting also nonionizable monomers), but only at the cost of a more complex synthetic procedure and with the risk of increasing polyelectrolyte hydrophobicity.

As a final example, one may consider that the possibility of fostering the adsorption of anion-coordinated polyacids onto positively charged surfaces may impart the latter with local acid−base buffering capability, the range of pH over which the latter is exerted somewhat depending on the interaction strength between anions and acid groups. In this respect, one may envisage to use the latter materials as a surface-localized proton bath, with polymeric chains adsorbing more tightly upon ionization, or to generate matrices for drug release responding to two alternative stimuli, namely, a change in proton chemical potential, via polyacid ionization, and an increase in solution ionic force, which would reduce the surface−chain interaction intensity.

APPENDIX. ΔA versus pH and c-H-Bond STRENGTH (ζ) FOR AN ELECTROLYTIC SYSTEM CONTAINING POLYACIDS

Apart from collecting distributions from MC configuration sampling to characterize polymer conformations and species distributions in our systems, useful thermodynamic data may also be obtained from our simulations. Of a particular relevance for the aim of our study, there are the change in Helmholtz energy of polyelectrolytes due to monomer ionization ($\Delta_{ion}A(pH^*)$) or to the donation of c-H-bonds to anions ($\Delta A(\zeta)$).

As for $\Delta_{ion}A(pH^*)$, we have previously proved that a relationship derived by Reed and Reed under simplifying assumption,[53] and relating the change in Helmholtz energy of a polyacid upon increasing the solution pH from a situation with $\alpha = 0$ to a desired pH* is *de facto* exact within the framework of the constant-pH ensemble.[58] In the context of the systems we aim to study, the relationship reads

$$\Delta_{ion}A(pH^*) = -\ln(10)2N_p\beta^{-1}\int_{pH\ll pK_a}^{pH^*}\alpha(pH)\,d(pH - pK_a) \quad (5)$$

with $\beta^{-1} = k_BT$, and represents the change in Helmholtz energy of a system containing N_p acid groups due to an increase of the pH from a extremely low value (so that $\alpha = 0$) to pH*. Obviously, the linear relationship $\lambda = pH - pK_a$ easily allows one to recast eq 5 in terms of λ. We have previously used such quantity to characterize polyelectrolytes energetics and adsorption spontaneity in several circumstances.[19,48,50,58,74,75]

As for gauging the impact on the systems Helmholtz energy due to c-H-bond formation, we recall that the chosen analytical form for the c-H-bond potential is indeed linear in the well depth ζ (see discussion in section 2.1), a fact that allows one a fairly easy estimate.[40] In our specific case, it is convenient to exploit thermodynamic integration,[76] increasing the well depth from zero to ζ^* to compute $\Delta_{MB}A(\zeta^*) = \int_0^{\zeta^*}\langle e(\rho)\rangle_\zeta\,d\zeta$, with $\langle e(\rho)\rangle_\zeta$ being the average number of c-H-bonds. The latter, obviously, depends on the interaction intensity itself, but it is a quantity for which is straightforward to tabulate values versus ζ via MC simulations; numerical integrals could thus be computed with appropriate integration formulas.

ASSOCIATED CONTENT

Supporting Information

The Supporting Information is available free of charge at https://pubs.acs.org/doi/10.1021/acs.macromol.1c02625.

Figures S1−S7 (PDF)

AUTHOR INFORMATION

Corresponding Author

Massimo Mella − *Dipartimento di Scienza ed Alta Tecnologia, Università degli Studi dell'Insubria, 22100 Como (I), Italy;* orcid.org/0000-0001-7227-9715; Email: massimo.mella@uninsubria.it

Author

Andrea Tagliabue − *Dipartimento di Scienza ed Alta Tecnologia, Università degli Studi dell'Insubria, 22100 Como (I), Italy;* orcid.org/0000-0001-9520-0627

Complete contact information is available at: https://pubs.acs.org/10.1021/acs.macromol.1c02625

Author Contributions

M.M. ideated the study; A.T. and M.M. wrote the simulation codes; M.M. executed the simulations and analyzed the results; M.M. and A.T. wrote the manuscript.

Notes

The authors declare no competing financial interest.

ACKNOWLEDGMENTS

M.M. thanks the Università degli Studi dell'Insubria for funding under the scheme Fondo d'Ateneo per la Ricerca (FAR2020). A.T. thanks the Università degli Studi dell'Insubria for a Ph.D. studentship (2017−2020).

REFERENCES

(1) Xu, Y.; Bolisetty, S.; Drechsler, M.; Fang, B.; Yuan, J.; Ballauff, M.; Müller, A. H. pH and salt responsive poly(N,N-dimethylaminoethyl methacrylate) cylindrical brushes and their quaternized derivatives. *Polymer* **2008**, *49*, 3957−3964.

(2) Trotsenko, O.; Roiter, Y.; Minko, S. Conformational Transitions of Flexible Hydrophobic Polyelectrolytes in Solutions of Monovalent and Multivalent Salts and Their Mixtures. *Langmuir* **2012**, *28*, 6037−6044.

(3) Wu, T.; Gong, P.; Szleifer, I.; Vlček, P.; Šubr, V.; Genzer, J. Behavior of Surface-Anchored Poly(acrylic acid) Brushes with Grafting Density Gradients on Solid Substrates: 1. Experiment. *Macromolecules* **2007**, *40*, 8756−8764.

(4) Currie, E. P. K.; Sieval, A. B.; Fleer, G. J.; Stuart, M. A. C. Polyacrylic Acid Brushes: Surface Pressure and Salt-Induced Swelling. *Langmuir* **2000**, *16*, 8324−8333.
(5) Zhang, J.; Cai, H.; Tang, L.; Liu, G. Tuning the pH Response of Weak Polyelectrolyte Brushes with Specific Anion Effects. *Langmuir* **2018**, *34*, 12419−12427.
(6) Tagliabue, A.; Izzo, L.; Mella, M. Interface Counterion Localization Induces a Switch between Tight and Loose Configurations of Knotted Weak Polyacid Rings despite Intermonomer Coulomb Repulsions. *J. Phys. Chem. B* **2020**, *124*, 2930−2937.
(7) Tagliabue, A.; Micheletti, C.; Mella, M. Tunable Knot Segregation in Copolyelectrolyte Rings Carrying a Neutral Segment. *ACS Macro Lett.* **2021**, *10*, 1365−1370.
(8) Qu, C.; Jing, B.; Wang, S.; Zhu, Y. Distinct Effects of Multivalent Macroion and Simple Ion on the Structure and Local Electric Environment of a Weak Polyelectrolyte in Aqueous Solution. *J. Phys. Chem. B* **2017**, *121*, 8829−8837.
(9) Jacobs, M.; Lopez, C. G.; Dobrynin, A. V. Quantifying the Effect of Multivalent Ions in Polyelectrolyte Solutions. *Macromolecules* **2021**, *54*, 9577−9586.
(10) Angelescu, D. G.; Stenhammar, J.; Linse, P. Packaging of a Flexible Polyelectrolyte Inside a Viral Capsid. Effect of Salt Concentration and Salt Valence. *J. Phys. Chem. B* **2007**, *111*, 8477−8485.
(11) Borukhov, I.; Andelman, D.; Borrega, R.; Cloitre, M.; Leibler, L.; Orland, H. Polyelectrolyte Titration: Theory and Experiment. *J. Phys. Chem. B* **2000**, *104*, 11027−11034.
(12) da Silva, F. L. B.; Bogren, D.; Söderman, O.; Åkesson, T.; Jönsson, B. Titration of Fatty Acids Solubilized in Cationic, Nonionic, and Anionic Micelles. Theory and Experiment. *J. Phys. Chem. B* **2002**, *106*, 3515−3522.
(13) Ullner, M.; Jönsson, B. A Monte Carlo Study of Titrating Polyelectrolytes in the Presence of Salt. *Macromolecules* **1996**, *29*, 6645−6655.
(14) Carnal, F.; Ulrich, S.; Stoll, S. Influence of Explicit Ions on Titration Curves and Conformations of Flexible Polyelectrolytes: A Monte Carlo Study. *Macromolecules* **2010**, *43*, 2544−2553.
(15) Ziebarth, J. D.; Wang, Y. Understanding the Protonation Behavior of Linear Polyethylenimine in Solutions through Monte Carlo Simulations. *Biomacromolecules* **2010**, *11*, 29−38.
(16) Uyaver, S.; Seidel, C. Effect of varying salt concentration on the behavior of weak polyelectrolytes in a poor solvent. *Macromolecules* **2009**, *42*, 1352−1361.
(17) Zito, T.; Seidel, C. Equilibrium charge distribution on annealed polyelectrolytes. *Eur. Phys. J. E* **2002**, *8*, 339−346.
(18) Ferrand-Drake del Castillo, G.; Hailes, R. L. N.; Dahlin, A. Large Changes in Protonation of Weak Polyelectrolyte Brushes with Salt Concentration—Implications for Protein Immobilization. *J. Phys. Chem. Lett.* **2020**, *11*, 5212−5218.
(19) Mella, M.; Tagliabue, A.; Mollica, L.; Izzo, L. Monte Carlo study of the Effects of Macroion Charge Distribution on the Ionization and Adsorption of Weak Polyelectrolytes and Concurrent Counterion release. *J. Colloid Interface Sci.* **2020**, *560*, 667−680.
(20) Mella, M.; Mollica, L.; Izzo, L. Influence of charged intramolecular hydrogen bonds in weak polyelectrolytes: A Monte Carlo study of flexible and extendible polymeric chains in solution and near charged spheres. *J. Polym. Sci., Part B: Polym. Phys.* **2015**, *53*, 650−663.
(21) Stornes, M.; Linse, P.; Dias, R. S. Monte Carlo Simulations of Complexation between Weak Polyelectrolytes and a Charged Nanoparticle. Influence of Polyelectrolyte Chain Length and Concentration. *Macromolecules* **2017**, *50*, 5978−5988.
(22) Landsgesell, J.; Nová, L.; Rud, O.; Uhlík, F.; Sean, D.; Hebbeker, P.; Holm, C.; Košovan, P. Simulations of ionization equilibria in weak polyelectrolyte solutions and gels. *Soft Matter* **2019**, *15*, 1155−1185.
(23) Stornes, M.; Shrestha, B.; Dias, R. PH-Dependent Polyelectrolyte Bridging of Charged Nanoparticles. *J. Phys. Chem. B* **2018**, *122*, 10237−10246.
(24) Carnal, F.; Stoll, S. Adsorption of Weak Polyelectrolytes on Charged Nanoparticles. Impact of Salt Valency, pH, and Nanoparticle Charge Density. Monte Carlo Simulations. *J. Phys. Chem. B* **2011**, *115*, 12007−12018.
(25) Ulrich, S.; Seijo, M.; Laguecir, A.; Stoll, S. Nanoparticle Adsorption on a Weak Polyelectrolyte. Stiffness, pH, Charge Mobility, and Ionic Concentration Effects Investigated by Monte Carlo Simulations. *J. Phys. Chem. B* **2006**, *110*, 20954−20964.
(26) Laguecir, A.; Stoll, S. Adsorption of a weakly charged polymer on an oppositely charged colloidal particle: Monte Carlo simulations investigation. *Polymer* **2005**, *46*, 1359−1372.
(27) Bai, L.; Li, E.; Du, Z.; Yuan, S. Structural changes of PMMA substrates with different electrolyte solutions: A molecular dynamics study. *Colloids Surf., A* **2017**, *522*, 51−57.
(28) Lages, S.; Lindner, P.; Sinha, P.; Kiriy, A.; Stamm, M.; Huber, K. Formation of Ca2+-Induced Intermediate Necklace Structures of Polyacrylate Chains. *Macromolecules* **2009**, *42*, 4288−4299.
(29) Schweins, R.; Lindner, P.; Huber, K. Calcium Induced Shrinking of NaPA Chains: A SANS Investigation of Single Chain Behavior. *Macromolecules* **2003**, *36*, 9564−9573.
(30) Nap, R. J.; Park, S. H.; Szleifer, I. Competitive calcium ion binding to end-tethered weak polyelectrolytes. *Soft Matter* **2018**, *14*, 2365−2378.
(31) Nap, R. J.; Gonzalez Solveyra, E.; Szleifer, I. The interplay of nanointerface curvature and calcium binding in weak polyelectrolyte-coated nanoparticles. *Biomater. Sci.* **2018**, *6*, 1048−1058.
(32) Schweins, R.; Goerigk, G.; Huber, K. Shrinking of anionic polyacrylate coils induced by Ca2+, Sr2+ and Ba2.: A combined light scattering and ASAXS study. *Eur. Phys. J. E* **2006**, *21*, 99−110.
(33) Lages, S.; Goerigk, G.; Huber, K. SAXS and ASAXS on Dilute Sodium Polyacrylate Chains Decorated with Lead Ions. *Macromolecules* **2013**, *46*, 3570−3580.
(34) Ezhova, A.; Huber, K. Specific Interactions of Ag+ Ions with Anionic Polyacrylate Chains in Dilute Solution. *Macromolecules* **2014**, *47*, 8002−8011.
(35) Andreozzi, P.; Ricci, C.; Porcel, J. E. M.; Moretti, P.; Di Silvio, D.; Amenitsch, H.; Ortore, M. G.; Moya, S. E. Mechanistic study of the nucleation and conformational changes of polyamines in the presence ofphosphate ions. *J. Colloid Interface Sci.* **2019**, *543*, 335−342.
(36) Cuenca, V. E.; Martinelli, H.; Ramirez, M. d. l. A.; Ritacco, H. A.; Andreozzi, P.; Moya, S. E. Polyphosphate Poly(amine) Nanoparticles: Self-Assembly, Thermodynamics, and Stability Studies. *Langmuir* **2019**, *35*, 14300−14309.
(37) Meot-Ner, M.; Elmore, D. E.; Scheiner, S. Ionic Hydrogen Bond Effects on the Acidities, Basicities, Solvation, Solvent Bridging, and Self-Assembly of Carboxylic Groups. *J. Am. Chem. Soc.* **1999**, *121*, 7625−7635.
(38) de Souza, V. V.; Carretero, G. P. B.; Vitale, P. A. M.; Todeschini, Í.; Kotani, P. O.; Saraiva, G. K. V.; Guzzo, C. R.; Chaimovich, H.; Florenzano, F. H.; Cuccovia, I. M. Stimuli-responsive polymersomes of poly [2-(dimethylamino) ethyl methacrylate]-b-polystyrene. *Polym. Bull.* **2021**, *165*, 112113.
(39) Brinatti, C.; Mello, L. B.; Loh, W. Thermodynamic Study of the Micellization of Zwitterionic Surfactants and Their Interaction with Polymers in Water by Isothermal Titration Calorimetry. *Langmuir* **2014**, *30*, 6002−6010.
(40) Mella, M.; Tagliabue, A.; Mollica, L.; Vaghi, S.; Izzo, L. Inducing pH control over the critical micelle concentration of zwitterionic surfactants via polyacids adsorption: Effect of chain length and structure. *J. Colloid Interface Sci.* **2022**, *606*, 1636−1651.
(41) Aoki, K.; Kakiuchi, T. pKa of an ω-carboxylalkanethiol self-assembled monolayer by interaction model. *J. Electroanal. Chem.* **1999**, *478*, 101−107.
(42) Liu, Y.-J.; Navasero, N. M.; Yu, H.-Z. Structure and Reactivity of Mixed ω-Carboxyalkyl/Alkyl Monolayers on Silicon: ATR-FTIR Spectroscopy and Contact Angle Titration. *Langmuir* **2004**, *20*, 4039−4050.

https://doi.org/10.1021/acs.macromol.1c02625
Macromolecules 2022, 55, 4533−4547

(43) Apel, C. L.; Deamer, D. W.; Mautner, M. N. Self-assembled vesicles of monocarboxylic acids and alcohols: conditions for stability and for the encapsulation of biopolymers. *Biochimica et Biophysica Acta (BBA) - Biomembranes* **2002**, *1559*, 1−9.
(44) Šturcová, A.; Dybal, J.; Braunová, A.; Pechar, M. Micellization-induced deprotonation of thermoresponsive surfactant CAE-85 — the telechelic carboxylic group derivative of Pluronic P85. *Vib. Spectrosc.* **2011**, *57*, 300−305.
(45) Smith, D. A.; Wallwork, M. L.; Zhang, J.; Kirkham, J.; Robinson, C.; Marsh, A.; Wong, M. The Effect of Electrolyte Concentration on the Chemical Force Titration Behavior of ω-Functionalized SAMs: Evidence for the Formation of Strong Ionic Hydrogen Bonds. *J. Phys. Chem. B* **2000**, *104*, 8862−8870.
(46) Tagliabue, A.; Izzo, L.; Mella, M. Impact of Charge Correlation, Chain Rigidity, and Chemical Specific Interactions on the Behavior of Weak Polyelectrolytes in Solution. *J. Phys. Chem. B* **2019**, *123*, 8872−8888.
(47) Wennerström, H.; Jönsson, B.; Linse, P. The cell model for polyelectrolyte systems. Exact statistical mechanical relations, Monte Carlo simulations, and the Poisson−ÄìBoltzmann approximation. *J. Chem. Phys.* **1982**, *76*, 4665−4670.
(48) Tagliabue, A.; Izzo, L.; Mella, M. Absorbed weak polyelectrolytes: Impact of confinement, topology, and chemically specific interactions on ionization, conformation free energy, counterion condensation, and absorption equilibrium. *J. Polym. Sci., Part B: Polym. Phys.* **2019**, *57*, 491−510.
(49) Mella, M.; Tagliabue, A.; Izzo, L. On the distribution of hydrophilic polyelectrolytes and their counterions around zwitterionic micelles: the possible impact on the charge density in solution. *Soft Matter* **2021**, *17*, 1267−1283.
(50) Mella, M.; Izzo, L. Modulation of ionization and structural properties of weak polyelectrolytes due to 1D, 2D, and 3D confinement. *J. Polym. Sci., Part B: Polym. Phys.* **2017**, *55*, 1088−1102.
(51) Pegado, L.; Marsalek, O.; Jungwirth, P.; Wernersson, E. Solvation and ion-pairing properties of the aqueous sulfate anion: explicit versus effective electronic polarization. *Phys. Chem. Chem. Phys.* **2012**, *14*, 10248−10257.
(52) Mella, M.; Izzo, L. Structural properties of hydrophilic polymeric chains bearing covalently-linked hydrophobic substituents: Exploring the effects of chain length, fractional loading and hydrophobic interaction strength with coarse grained potentials and Monte Carlo simulations. *Polymer* **2010**, *51*, 3582−3589.
(53) Reed, C. E.; Reed, W. F. Monte Carlo study of titration of linear polyelectrolytes. *J. Chem. Phys.* **1992**, *96*, 1609−1620.
(54) Landsgesell, J.; Holm, C.; Smiatek, J. Simulation of weak polyelectrolytes: a comparison between the constant pH and the reaction ensemble method. *European Physical Journal Special Topics* **2017**, *226*, 725−736.
(55) Labbez, C.; Jonsson, B. A new Monte Carlo method for the titration of molecules and minerals. *Lecture Notes in Computer Science (including subseries Lecture Notes in Artificial Intelligence and Lecture Notes in Bioinformatics)* **2007**, *4699 LNCS*, 66−72.
(56) Notice that C_s = 0.0059 M was chosen to compare with results on zwitterionic micelle−polyacid interactions,[40] as it corresponds to the equivalent salt concentration that would be present if all charged moieties in the headgroups of a micelle composed of 59 dodecyl sulfobetaines were allowed to roam freely. C_s = 0.01 and 0.02 M were instead chosen with the intention of investigating salts concentrations compatible with the one present in isotonic saline solutions.
(57) Ullner, M.; Woodward, C. E. Simulations of the Titration of Linear Polyelectrolytes with Explicit Simple Ions: Comparisons with Screened Coulomb Models and Experiments. *Macromolecules* **2000**, *33*, 7144−7156.
(58) Tagliabue, A.; Izzo, L.; Mella, M. Impact of Charge Correlation, Chain Rigidity, and Chemical Specific Interactions on the Behavior of Weak Polyelectrolytes in Solution. *J. Phys. Chem. B* **2019**, *123*, 8872−8888.
(59) Carnal, F.; Stoll, S. Chain stiffness, salt valency, and concentration influences on titration curves of polyelectrolytes: Monte Carlo simulations. *J. Chem. Phys.* **2011**, *134*, 044909.
(60) Ulrich, S.; Laguecir, A.; Stoll, S. Titration of hydrophobic polyelectrolytes using Monte Carlo simulations. *J. Chem. Phys.* **2005**, *122*, 094911.
(61) Uyaver, S.; Seidel, C. First-order conformational transition of annealed polyelectrolytes in a poor solvent. *Europhys. Lett.* **2003**, *64*, 536.
(62) Uyaver, S.; Seidel, C. Pearl-necklace structures in annealed polyelectrolytes. *J. Phys. Chem. B* **2004**, *108*, 18804−18814.
(63) Uhlík, F.; Košovan, P.; Limpouchová, Z.; Procházka, K.; Borisov, O.; Leermakers, F. Modeling of ionization and conformations of starlike weak polyelectrolytes. *Macromolecules* **2014**, *47*, 4004−4016.
(64) Yadav, V.; Harkin, A. V.; Robertson, M. L.; Conrad, J. C. Hysteretic memory in pH-response of water contact angle on poly(acrylic acid) brushes. *Soft Matter* **2016**, *12*, 3589−3599.
(65) Izzo, L.; Griffiths, P. C.; Nilmini, R.; King, S. M.; Wallom, K.-L.; Ferguson, E. L.; Duncan, R. Impact of polymer tacticity on the physico-chemical behaviour of polymers proposed as therapeutics. *Int. J. Pharm.* **2011**, *408*, 213−222.
(66) As a side note, we also point out that the shorter average distance between anions coordinated to $\mathcal{L}(1, 60, A)$ should also lower the dissociation probability at low α values compared to other species due to the higher average charge density and, hence, stronger like-charge repulsion. This effect is clearly evidenced in the ionization curves, with $\mathcal{L}(1, 60, A)$ passing the α = 0.01 threshold half a pH unit later than $\mathcal{L}(6, 10, A)$ (Figure S3), while the ionization of longer chains usually deviates from the one of shorter species only above α = 0.02−0.03.[19,40]
(67) Wallin, T.; Linse, P. Monte Carlo Simulations of Polyelectrolytes at Charged Micelles. 1. Effects of Chain Flexibility. *Langmuir* **1996**, *12*, 305−314.
(68) Wallin, T.; Linse, P. Monte Carlo Simulations of Polyelectrolytes at Charged Micelles. 2. Effects of Linear Charge Density. *J. Phys. Chem.* **1996**, *100*, 17873−17880.
(69) Wallin, T.; Linse, P. Monte Carlo Simulations of Polyelectrolytes at Charged Micelles. 3. Effects of Surfactant Tail Length. *J. Phys. Chem. B* **1997**, *101*, 5506−5513.
(70) Goswami, M.; Borreguero, J. M.; Pincus, P. A.; Sumpter, B. G. Surfactant-Mediated Polyelectrolyte Self-Assembly in a Polyelectrolyte,ÀìSurfactant Complex. *Macromolecules* **2015**, *48*, 9050−9059.
(71) Li, D.; Wagner, N. J. Universal Binding Behavior for Ionic Alkyl Surfactants with Oppositely Charged Polyelectrolytes. *J. Am. Chem. Soc.* **2013**, *135*, 17547−17555.
(72) Gradzielski, M.; Hoffmann, I. Polyelectrolyte-surfactant complexes (PESCs) composed of oppositely charged components. *Curr. Opin. Colloid Interface Sci.* **2018**, *35*, 124−141.
(73) Li, D.; Kelkar, M. S.; Wagner, N. J. Phase Behavior and Molecular Thermodynamics of Coacervation in Oppositely Charged Polyelectrolyte/Surfactant Systems: A Cationic Polymer JR 400 and Anionic Surfactant SDS Mixture. *Langmuir* **2012**, *28*, 10348−10362.
(74) Mella, M.; Tagliabue, A.; Izzo, L. On the Distribution of Hydrophilic Polyelectrolytes and their Counterions around Zwitterionic Micelles: the Possible Impact on the Charge Density in Solution. *Soft Matter* **2021**, *17*, 12671283.
(75) Mella, M.; Tagliabue, A.; Vaghi, S.; Izzo, L. Evidences for charged hydrogen bonds on surfaces bearing weakly basic pendants: The case of PMMA-ran-PDMAEMA polymeric films. *Colloids Surf., A* **2021**, *620*, 126525.
(76) Kirkwood, J. G. Statistical Mechanics of Fluid Mixtures. *J. Chem. Phys.* **1935**, *3*, 300−313.

https://doi.org/10.1021/acs.macromol.1c02625
Macromolecules 2022, 55, 4533−4547